Climate Dynamics
https://doi.org/10.1007/s00382-018-4436-4

New findings on the route of heat transport between the Indo-Pacific and Southern Ocean

Enhui Liao[1,2] · Xiao-Hai Yan[2,3] · Yuwu Jiang[4] · Autumn N. Kidwell[5]

Received: 31 May 2018 / Accepted: 6 September 2018

Abstract
Since the end of the twentieth century, the global mean surface temperature (GMST) exhibited a shift from a rapid warming to an unexpected deceleration. An anomalous heat was transported from the Pacific Ocean into the Indian Ocean through a strengthened Indonesian Throughflow during the same period. Within this background, it is essential to continue tracking the fate of the anomalous heat arriving in the Indian Ocean to form a comprehensive picture of the global ocean energy redistribution. The anomalous heat may continue flowing westward into the Atlantic Ocean along the main pathway of the regional ocean currents via the South Equatorial Current (SEC) and Agulhas Current. However, here we examine an alternate pathway: a southward heat transport in conjunction with a weakened SEC, diverting the canonical westward transport. This additional transport pathway causes an increase in heat content in the South Indian Ocean mid-latitudes (15–30°S, 95–110°E), may contribute to the Southern Ocean warming, and intensifies hemispheric asymmetry of oceanic heat content. The heat increase has important climate impacts such as changes to rainfall and increased coral bleaching over the western coast of Australia. The new path discovered here may be an essential route of heat transport linking the tropical Indo-Pacific Ocean and the Southern Ocean in 2003–2012.

1 Introduction

The shift in global mean surface temperature (GMST) during 1998–2013 is a surface phenomenon and does not represent a slowdown in warming of the climate system but rather is an energy redistribution within the oceans (Yan et al. 2016). It has been shown that the change was induced by the heat sequestration from the atmosphere into the upper layer of equatorial Pacific via strengthened trade winds (England et al. 2014; Kosaka and Xie 2013; Trenberth and Fasullo 2013), and then the sequestered heat flowed westward into the upper ocean in the Indian Ocean through strengthened Indonesian Throughflow (ITF, Lee et al. 2015; Liu et al. 2016; Nieves et al. 2015). The reduction of GMST warming rate is also called global surface warming hiatus (Easterling and Wehner 2009), originally thought to indicate a reduction in global warming, which is a widely used phrase used to describe the deceleration in global surface warming. This nomenclature is continued herein to be consistent with previous studies. As a possible response to the surface warming hiatus, the recent global ocean heat trend pattern features an intensifying hemispheric asymmetry with 67–98% heat gain occurred in the southern hemisphere extra-tropical ocean and a large accumulation of heat in the mid-latitudes of

Electronic supplementary material The online version of this article (https://doi.org/10.1007/s00382-018-4436-4) contains supplementary material, which is available to authorized users.

✉ Xiao-Hai Yan
xiaohai@udel.edu

✉ Yuwu Jiang
ywjiang@xmu.edu.cn

1 Geosciences Department, Princeton University, Princeton, NJ, USA

2 College of Earth, Ocean and Environment, University of Delaware, Newark, DE, USA

3 University of Delaware/Xiamen University's Joint Center for Remote Sensing and Joint Institute for Coastal Research and Management, University of Delaware/Xiamen University, Newark, USA

4 State Key Laboratory of Marine Environmental Science, Xiamen University, Xiamen, China

5 Applied Research Laboratories, University of Texas at Austin, Austin, TX, USA

Published online: 17 September 2018

Southeast Indian Ocean (SEIO, Levitus et al. 2012; Roemmich et al. 2015; Wijffels et al. 2016). The Indian Ocean accounts for a large portion of the global ocean (0–700 m) heat gain via the strengthened ITF (Lee et al. 2015) and may have an important contribution to the hemispheric asymmetry during the global energy redistribution. The fate of the anomalous heat inflowing from strengthened ITF and the associated changes in the regional heat distribution in the Indian Ocean are still not well-understood. In this study, we investigate the OHC_{700} variability and the associated physical processes in the Indian Ocean by using a surface-forced global ocean circulation model (Community Earth System Model, CESM). The surface forcing is JRA55-do which is a new dataset and plans to replace the current Coordinated Ocean–ice Reference Experiments (CORE) dataset (Tsujino et al. 2018). The CESM is a state-of-art global climate model and the ocean–sea ice grid is on a displaced pole grid at a resolution of approximate 1° in the ocean with 60 vertical levels (Danabasoglu et al. 2012; Gent et al. 2011). Since the anomalous heat transport from the Pacific to the Indian Ocean was reported in 2003–2012 by Lee et al. (2015), we also focus on the period in 2003–2012.

2 Results

2.1 Ocean heat content variability and heat budget

In the SEIO, the OHC_{700} trend over 2003–2012 shows a prominent meridional band with a positive trend in heat content and the Southwest Indian Ocean (SWIO) has a negatively trended zonal band on the same period (Fig. 1a). In order to study the transfer of heat in the Indian Ocean, we divide the Indian Ocean into the North Indian Ocean (NIO, 0–25°N, 25–125°E), the SEIO (0–34°S, 25–76°E), and the SWIO (0–34°S, 76–125°E), which are defined in the supplementary Fig. s1. The positively trended meridional OHC band extends along the western coast of Australia from the equator to 40°S and the negatively trended zonal OHC band spreads along 15°S from Africa to the middle of the Indian Ocean (85°E). When the heat flows from the Pacific into the Indian Ocean, we expect a zonal heat transport along the main pathway of the South Equatorial Current (SEC) from the ITF region to the eastern coast of Africa (Lee et al. 2015), but, instead, there is an anomalous heat closer to Western Australia, implying some processes driving a southward transport within the Indian Ocean. The OHC trends in the NIO are weak, but show an energy balance with the cooling Arabian Sea and the warming Bay of Bengal. The heat content trend is not sensitive to the end points of the trend analysis indicating the observed trend in the Indian Ocean is a decadal timescale change (Supplementary Fig. s2). The heat trend patterns simulated by the CESM (Fig. 1b) are in good agreement with observation (Levitus et al. 2012), suggesting the CESM has captured major physical processes that determine the OHC_{700} variability. The time series of the OHC_{700} changes in the SEIO reveal an unusual rise in the 2000s, in contrast to OHC_{700} in the NIO and SWIO (Supplementary Fig. s3). The time series of the OHC_{700} in the SEIO grew persistently in the last decade, i.e., 2003–2012, while the OHC_{700} in the SWIO demonstrated a negative trend from 2008 to 2012. The spatial pattern and time series results imply most of the

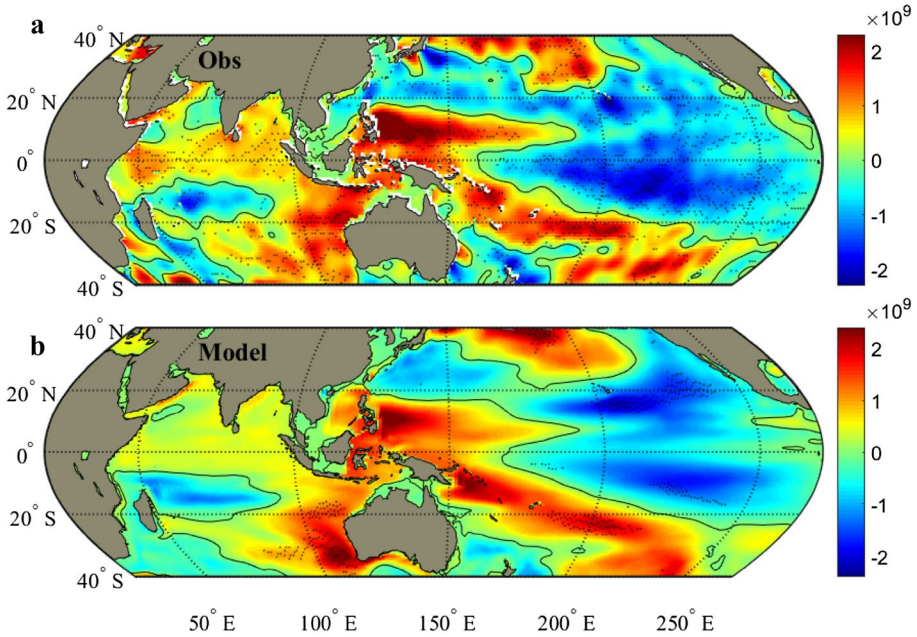

Fig. 1 The OHC_{700} linear trends (units: J/m^2/Decade) during the warming hiatus period (2003–2012) in the upper ocean (0–700 m). The black contour line is shown for 0. **a** The observation data is from Levitus et al. (2012). **b** The model result is from the CESM model. Black points in the shading color indicate the trends in those locations are significant in statistics ($P < 0.05$, significance test method referred to appendix)

anomalous heat carried by the ITF is accumulated in the SEIO and spreads southward off the western coast of Australia toward the Southern Ocean.

The mechanisms for the anomalous heat gain in the SEIO can be evaluated by comparing the heat budget terms in 2003–2012 with period computed as anomalies relative to the reference period (1990–2002). The heat budget includes four terms: storage rate, horizontal heat advection, vertical heat advection, and net surface heat flux. The storage rate is considered as the change of heat in the SEIO and determined by the other three terms (horizontal heat advection, vertical heat advection, and net surface heat flux). In Fig. 2a, the horizontal heat advection term almost follows the storage rate term which indicates the simulated increase of OHC_{700} was dominated by an intensified horizontal heat advection. The other two terms (vertical heat advection and net surface heat flux) remain around zero and contribute little to the storage rate term. This horizontal advection anomaly can be as high as 0.05 PW in 2003–2012 and is damped slightly by both the vertical heat advection and net surface heat flux. The total heat budget is shown in the supplementary Fig. S4. Further heat advection analysis (Fig. 2b) indicates that the increased horizontal heat advection is due to an increased heat inflow through the eastern (0.098 ± 0.056 PW/decade, positive trend means heat flux into the box) and the western (0.13 ± 0.057 PW/decade) boundaries in the SEIO. The sections for the heat transport are plotted as a white box in the Fig. 3a. The northern (− 0.17 ± 0.05 PW/decade, negative trend means heat outflow in the box) and southern (− 0.032 ± 0.029 PW/decade) borders show a rising heat outflow, but cannot compensate for the inflow in the other two borders.

The transports along the eastern and western borders are related to the ITF and SEC system respectively. The intensified heat inflow in the eastern border evidently relates to the recently strengthened ITF agreed with observations (Lee et al. 2015; Liu et al. 2015; Susanto et al. 2012). The strengthened ITF is driven by a strong anomalous pressure gradient formed from the tropical northwestern Pacific to the tropical South Indian Ocean (Lee et al. 2015). The anomalous surface wind and westward migration of wind convergence zone may be responsible for the pressure gradient (Kidwell et al. 2016; Lee and McPhaden 2008). The increased heat transport into the western boundary coincides with a reduced volume transport of SEC (Supplementary Fig. s4). This suggests a reduced heat outflow by a weakened SEC. The corresponding flow pattern will be analyzed in the following. A middle section (advM in Fig. 2b) between

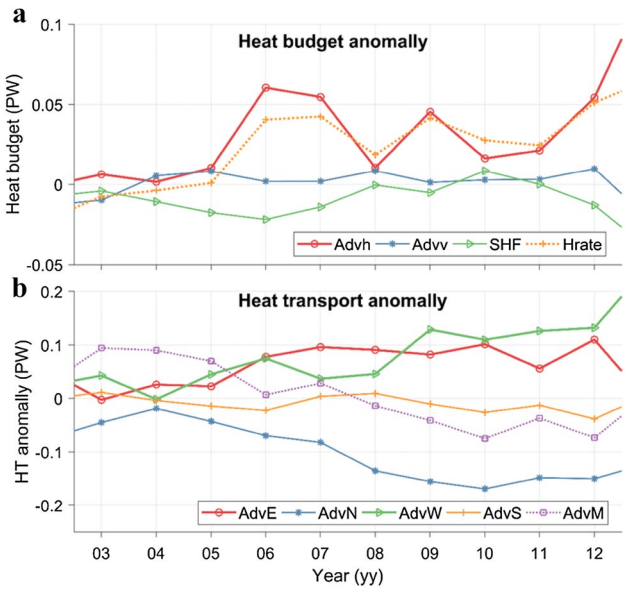

Fig. 2 The time series of heat budget anomalies (**a**) and heat transport anomalies (**b**) in the SEIO. **a** Storage rate (Hrate), horizontal heat advection (Advh), vertical heat advection (Advv), and net surface heat flux (SHF) for the SEIO. **b** The heat transport in the east (AdvE), north (AdvN), west (AdvW), south (AdvS) boundary of the SEIO and the AdvM is the heat transport cross the middle latitude in the SEIO. Anomalies relate to the reference period in 1990–2002. Heat increase (positive trend) is inflowing into the box and heat decrease (negative trend) is outflowing of the box. The section locations are plotted as white box in the Fig. 3a. PW is 10^{15} J/s

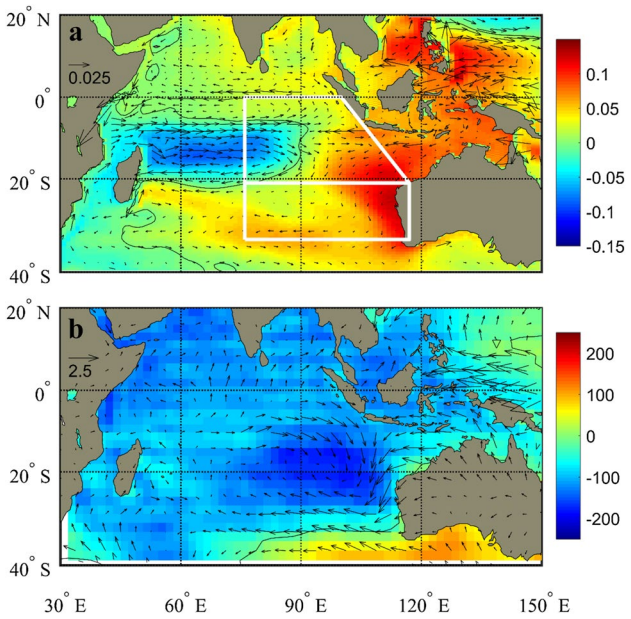

Fig. 3 **a** The linear trends for the depth-averaged (0–700 m) velocity (**a** vector, m/s/decade), sea level (**a** shading, m/decade), 10 m-wind (**b** vector, m/s/decade), and sea level pressure (**b** shading, Pa/decade) during the warming hiatus period (2003–2012). The velocity and sea level trends in **a** are from CESM model result. The white box is the line for the computation of volume transport and heat transport in the Fig. 2. The wind and sea level pressure trends in **b** are from JRA55-do atmospheric reanalysis data that drive the CESM. The black contour line is shown for 0

tropical and subtropical Indian Ocean (section location is in the Fig. 3a) is selected to illustrate the strength of southward transport from the tropic to the mid-latitudes in the SEIO. Note that the middle section (advM in Fig. 2b) indicates a strengthened southward heat flow with a rate of -0.2 ± 0.046 PW/decade (negative trend means heat outflow from the tropic to the mid-latitudes), which is stronger than the northern border (-0.17 ± 0.05 PW/decade) and the southern border (-0.032 ± 0.029 PW/decade). This suggests a large portion of the heat inflow from the eastern border moves southward and remains in the mid-latitudes and some heat continues moving southward. The heat transport variations are consistent with the water volume transport changes (Supplementary Fig. s4). The strengthened ITF moves plenty of anomalous heat into the SEIO, but a weakened outflow cannot deliver these anomalous heats out through the western side. Most of the anomalous heat shifts southward and remains in the mid-latitudes (20–30°S).

2.2 Sea level, circulation and wind trends

Given the important role played by the ITF and SEC systems, closer examinations of the depth-averaged velocity (0–700 m) and sea level are warranted (Fig. 3a). Eastward and westward current trends emerge in the western and eastern tropical Indian Ocean, respectively. These two anomalous flows converge around 90°E, then most of the anomalous flows turn southward and part of them turn northward to the NIO. The location of anomalous eastward current coincides with the SEC which implies the SEC is weakened. Stemmed from the southward turning, a strengthened southward flow is witnessed from the equator to the 34°S in the SEIO, which is consistent with a recent increase in the strength of pole-ward Leeuwin Current (Feng et al. 2015).

Corresponding to the flow trend, the sea level trend reveals zonal-negative and meridional-positive bands in the equatorial region in the SWIO and along the western coast of Australia in the SEIO respectively (Fig. 3a) which match the OHC_{700} pattern. The zonal-negative sea level trend results in a southward sea level gradient, covering a region from the eastern coast of Africa to the 90°E and from -5°S to -17°S. This suggests that the negative sea level trend may weaken the western part of SEC through a latitudinal sea level gradient in the SWIO. The meridional-positive sea level trend leads to a westward sea level gradient, spanning from the equator to the 40°S along the coast of Western Australia. The westward sea level gradient may strengthen a southward flow that connects the ITF and the mid-latitudes of South Indian Ocean. The velocity variabilities mostly emerge in the surface layer (supplementary Fig. s5) which reaffirms that the weakened SEC and strengthened southward current are associated with the surface sea level variations.

The sea level variability at decadal time scale in the Indian Ocean is largely explained by the wind variation in the tropical and sub-tropical Indo-Pacific in terms of the Ekman pumping and the planetary waves (Feng et al. 2010; Nidheesh et al. 2013; Timmermann et al. 2010). The sea level and wind trends in the Fig. 3 illustrate similar responses with previous studies (Han et al. 2010; Lee and McPhaden 2008; Nidheesh et al. 2013). The location (5°S–20°S) of a zonal drop of sea level is consistent with Southern Hemisphere Ekman mass transport to the left of the surface westerly wind trend (Fig. 3b). In addition, the time evolution of this zonal drop of sea level (Supplementary Fig. s6) shows a westward propagation of sea level drop suggesting a contribution of oceanic Rossby waves to the development and propagation of the drop. The Rossby waves are driven by the wind stress curl through Ekman pumping (Supplementary Fig. s7) which is specified by Han et al. (2010), Lee and McPhaden (2008), and Nidheesh et al. (2013). The sea level variations in the SWIO (5°S–20°S) and tropical Pacific are negatively correlated with each other as are trade wind variation across two basins. The negative correlation may be associated with a change of deep convection associated with the Walker circulation over the tropical Pacific and Indian Oceans (Han et al. 2010), which is consistent with the recent La Niña-like state in the Pacific.

In the SEIO, the positive sea level trend is related to the northerly wind anomalies off the Western Australia coast (Fig. 3b) and a transmission of the high sea level signals from Pacific via the equatorial and coastal waveguides. The northerly wind anomalies as part of the cyclonic wind anomalies are caused by a negative sea level pressure anomalies (Fig. 3b) due to a Gill response to the La Niña (Feng et al. 2013). The cyclonic wind anomalies are also partly strengthened by the local ocean–atmosphere interaction that the northerly wind anomalies induce positive SST anomalies by suppressing latent heat loss and strengthening the warm water advection (Feng et al. 2013; Tozuka et al. 2014). The high sea level signals propagating as coastal Kelvin wave result from recently strengthening of trade winds and associated wind stress curls in the Pacific (England et al. 2014; Nidheesh et al. 2013). The transmission is accompanied by an increased ITF transport as indicated by Feng et al. (2010). As a result, the weakened SEC is related to the westerly wind anomalies and related wind stress curl while the strengthened southward current is linked to the cyclonic wind anomalies and sea level anomalies transmission from Pacific as a response to the La Niña like-state in the Pacific.

3 Model experiments

The conjunction between flow and wind trend patterns indicates the wind variability is responsible for the flow variation and heat redistribution in 2003–2012. In order to further

verify the role of wind and sea level variability, we conduct a numerical experiment, named as IOclim that the Indian Ocean is driven by the climatological wind while the other ocean basins are still driven by the realistic wind. In contrast to the control case (all realistic wind), the OHC_{700} in the IOclim (Fig. 4a) is characterized by a zonal band instead of a meridional band. The anomalous OHC_{700} extends from the eastern tropical Indian Ocean to the western tropical Indian Ocean along the path of the SEC. The sea level trend (Fig. 4b) has a similar westward expansion with the OHC_{700}. An intensified westward flow emerges in the tropical region connecting the eastern and western tropical Indian Ocean. This is an expected heat pathway via the strengthened SEC and Agulhas current. Note that the IOclim case still has a warming trend in the mid-latitudes (western coast of Australia), but a less rate than that of the control case. The reason is the existence of high sea level transmission from the Pacific, even though wind anomalies vanish in the IOclim case. The test result confirms the above conclusion that the weakened westward heat transport and strengthened southward heat transport observed are largely dominated by the wind and sea level variability during the "hiatus" period. The zonally integrated heat gain in the Indian Ocean (Fig. 4c) indicates most of the anomalous heat is accumulated in the tropical Indian Ocean (15°S) in the IOclim case instead of mid-latitudes (32°S) in the control case. For the global energy redistribution, the heat gain versus latitude (Fig. 4d) implies that the IOclim case tends to keep the heat into the Indian Ocean while the control case moves some of the anomalous heat southward to the Southern Ocean (south to 33.5°S, region is defined in Fig. S1). As a consequence, the Southern Ocean experiences a slight higher warming rate in the control case ($1.57\times10^{22}\pm1.20\times10^{21}$ J/decade) than that in the IOclim case ($1.50\times10^{22}\pm1.02\times10^{21}$ J/decade, supplementary Fig. s8). However, the warming rate of Southern Ocean in the IOclim case may vary with a change of border between climatological wind in the Indian Ocean and realistic wind in the Southern Ocean. Further study of the detailed influence on the Southern Ocean is needed. Although relatively small variability with a rate of 5% in the experiment, this may partly contribute a recently rapid warming of the Southern Ocean which is reported by many studies (Riser et al. 2016; Sutton and Roemmich 2011). This reaffirms that the strengthened-southward heat transport not only builds up heat in the middle latitudes of South Indian Ocean but also contributes to the warming Southern Ocean and global energy redistribution within the oceans.

4 Summary and discussion

The consistent changes of observed/simulated sea level and atmospheric circulation show that the strengthened southward heat transport in the Indian Ocean is a

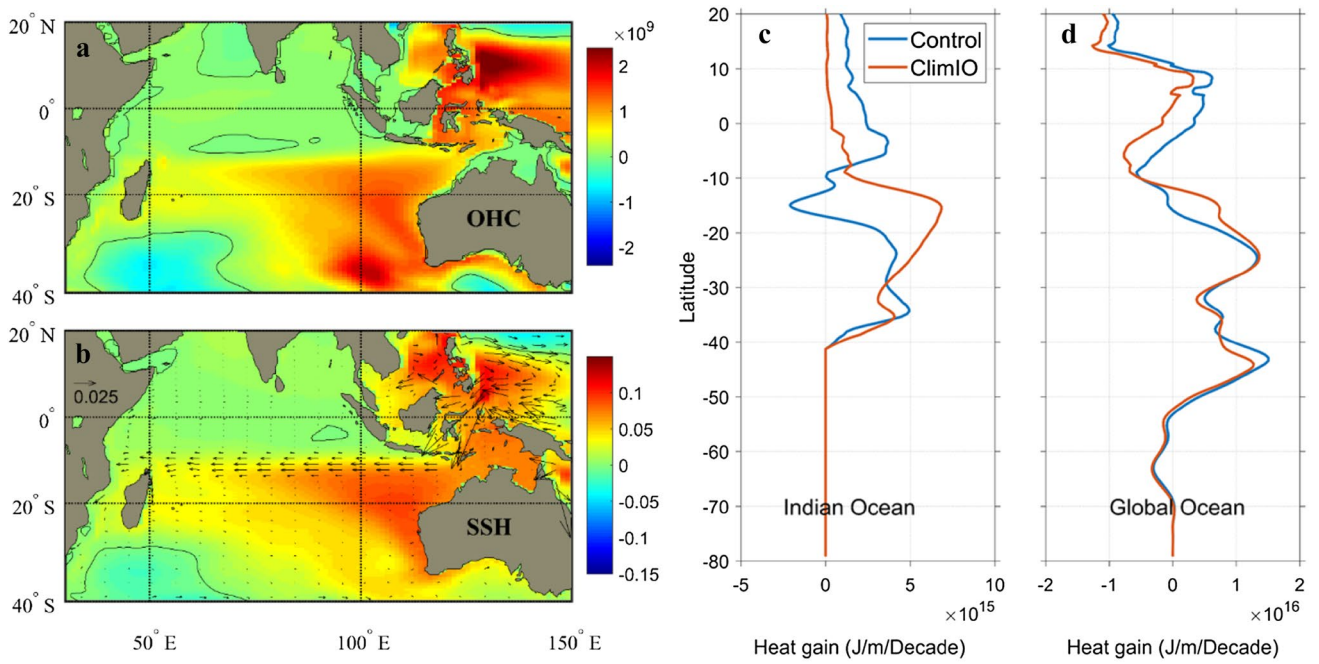

Fig. 4 **a** The The OHC_{700} linear trends (units: J/m^2/Decade) for the IOclim case during the warming hiatus (2003–2012) that the Indian Ocean is driven by climatological wind. **b** Depth-averaged velocity (0–700 m, m/s/decade) and sea level (m/decade) linear trends for the IOclim case (2003–2012). **c, d** Zonally integrated heat gain versus latitude in the Indian Ocean and global ocean respectively. The results are from the IOclim case. The black contour lines in **a** and **b** are shown for 0

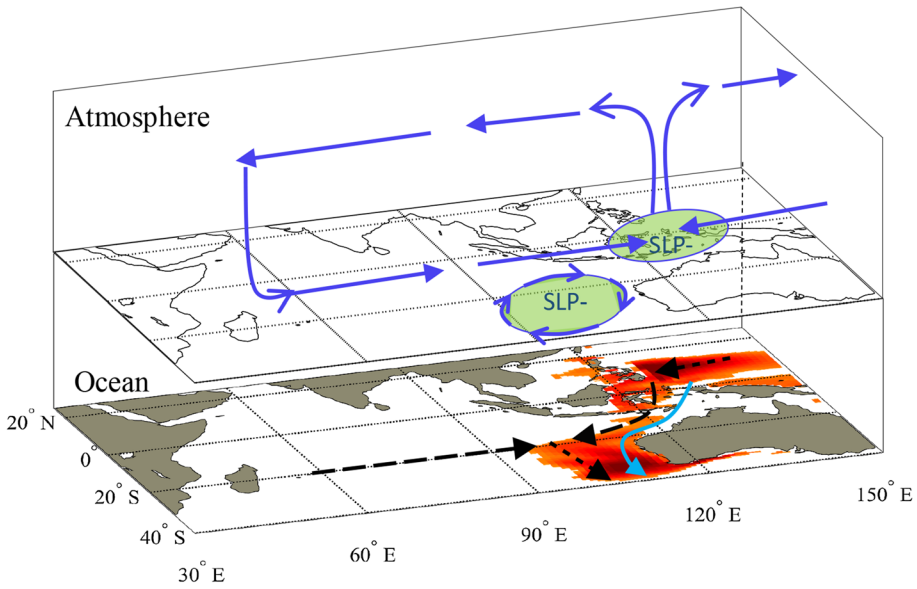

Fig. 5 The schematic graph of the trends in OHC_{700} and ocean–atmosphere circulation in the Indo-Pacific over 2003–2012. The color shading represents the OHC_{700} trend (red represents warming). In the atmosphere part, the blue solid vector is the wind anomaly under the influence of La Niña-like state in the Pacific Ocean. The "SLP-" means the negative sea level pressure trend. In the ocean part, the dashed black vectors are the flow trend and the green solid vector is the transmission of high sea level from the Pacific to the Indian Ocean

consequence of the La Niña state in the Pacific during the surface warming hiatus. The mechanism and significance are summarized in Fig. 5. Under the influence of the La Niña-like state in the Pacific, according to Gill response, the westerly wind anomalies are induced in the SWIO and cyclonic wind anomalies and a high sea level anomaly are formed in the SEIO during the surface warming hiatus. The westerly wind anomalies weaken the SEC while the cyclonic wind anomalies and a high sea level anomaly strengthens a southward flow. As a result, the anomalous heat from the Pacific moves southward through the strengthened southward flow instead of flowing westward by the weakened SEC.

The heat path detailed here may be an important path linking the tropical Indo-Pacific and the Southern Ocean during the La Niña. Compared with the traditional path (SEC and Agulhas Current), this path is short indicating a fast-poleward heat transport. The response between the tropical Indo-Pacific and Southern Oceans through oceanic-teleconnection may be quicker than we thought before. The strengthened southward heat transport has important climate impacts such as changed rainfall over the western coast of Australia and increased coral bleaching (Feng et al. 2013; Ummenhofer et al. 2015; Zinke et al. 2015). The anomalous heat not only moves southward to the Southern Ocean, but also flows eastward along the southern coast of Australia through the Leeuwin Current (Fig. 1). A rapid surface warming was observed in this coastal region during the "hiatus" period (Liao et al. 2015) suggesting a rising probability of occurrence of a hot event. Therefore, monitoring and predicting the continuing changes of the strengthened southward heat transport in the Indian Ocean remain among key priorities.

Acknowledgements Authors would like to thank Dr. Stephen G. Yeager and Dr. Who Kim from NCAR for the help in the CESM model running. The research was partially supported by SOA Global Change and Air-Sea Interaction Project (GASI-IPOVAI-01-04, GASI-02-PAC-YGST2-02) and National Natural Science Foundation of China (41630963 and 41476007). We would also like to thank the Delaware Space and Sea Grant (NNX15AI19H and Na14OAR4170087) for financial support.

References

Danabasoglu G et al (2012) The CCSM4 ocean component. J Clim 25:1361–1389

Easterling DR, Wehner MF (2009) Is the climate warming or cooling? Geophys Res Lett 36:L08706. https://doi.org/10.1029/2009gl037810

England MH et al (2014) Recent intensification of wind-driven circulation in the Pacific and the ongoing warming hiatus. Nature Clim Change 4:222–227. https://doi.org/10.1038/nclimate2106

Feng M, McPhaden MJ, Lee T (2010) Decadal variability of the Pacific subtropical cells and their influence on the southeast. Indian Ocean Geophys Res Lett 37:L09606. https://doi.org/10.1029/2010GL042796

Feng M, McPhaden MJ, Xie SP, Hafner J (2013) La Nina forces unprecedented Leeuwin Current warming in 2011. Sci Rep 3:1277. https://doi.org/10.1038/srep01277

Feng M et al (2015) Decadal increase in NingalooNiñosince the late 1990. Geophys Res Lett 42:104–112. https://doi.org/10.1002/2014gl062509 s

Gent PR et al (2011) The community climate system model version 4. J Clim 24:4973–4991. https://doi.org/10.1175/2011JCLI4083.1

Han W et al (2010) Patterns of Indian Ocean sea-level change in a warming climate. Nature Geosci 3:546–550. https://doi.org/10.1038/ngeo901

Kidwell A, Lee T, Jo Y-H, Yan X-H (2016) Characterization of the variability of the South Pacific convergence zone using satellite and reanalysis wind products. J Clim 29:1717–1732

Kosaka Y, Xie SP (2013) Recent global-warming hiatus tied to equatorial Pacific surface cooling. Nature 501:403–407. https://doi.org/10.1038/nature12534

Lee T, McPhaden MJ (2008) Decadal phase change in large-scale sea level and winds in the Indo-Pacific region at the end of the 20th century. Geophys Res Lett 35:L01605. https://doi.org/10.1029/2007gl032419

Lee S-K, Park W, Baringer MO, Gordon AL, Huber B, Liu Y (2015) Pacific origin of the abrupt increase in Indian Ocean heat content during the warming hiatus. Nature Geosci 8:445–449. https://doi.org/10.1038/ngeo2438

Levitus S et al (2012) World ocean heat content and thermosteric sea level change (0–2000 m), 1955–2010 Geophys Res Lett 39 https://doi.org/10.1029/2012gl051106

Liao EH, Lu WF, Yan X-H, Jiang YW, Kidwell A (2015) The coastal ocean response to the global warming acceleration and hiatus. Sci Rep 5:16630. https://doi.org/10.1038/srep16630

Liu Q-Y, Feng M, Wang D, Wijffels S (2015) Interannual variability of the Indonesian throughflow transport: a revisit based on 30 year expendable bathythermograph data. J Geophys Res Oceans 120:8270–8282. https://doi.org/10.1002/2015JC011351

Liu W, Xie S-P, Lu J (2016) Tracking ocean heat uptake during the surface warming hiatus. Nat Commun. https://doi.org/10.1038/ncomms10926

Nidheesh AG, Lengaigne M, Vialard J, Unnikrishnan AS, Dayan H (2013) Decadal and long-term sea level variability in the tropical Indo-Pacific. Ocean Clim Dyn 41:381–402. https://doi.org/10.1007/s00382-012-1463-4

Nieves V, Willis JK, Patzert WC (2015) Recent hiatus caused by decadal shift in Indo-Pacific heating. Science 349:532–535

Riser SC et al (2016) Fifteen years of ocean observations with the global Argo array. Nature Clim Change 6:145–153. https://doi.org/10.1038/nclimate2872

Roemmich D, Church J, Gilson J, Monselesan D, Sutton P, Wijffels S (2015) Unabated planetary warming and its ocean structure since 2006. Nature Clim Change 5:240–245. https://doi.org/10.1038/nclimate2513

Susanto RD, Ffield A, Gordon AL, Adi TR (2012) Variability of Indonesian throughflow within Makassar Strait, 2004–2009. J Geophys Res Oceans 117:C09013. https://doi.org/10.1029/2012JC008096

Sutton P, Roemmich D (2011) Decadal steric and sea surface height changes in the Southern Hemisphere. Geophys Res Lett 38:L08604. https://doi.org/10.1029/2011GL046802

Timmermann A, McGregor S, Jin F-F (2010) Wind effects on past and future regional sea level trends in the southern Indo-Pacific. J Clim 23:4429–4437. https://doi.org/10.1175/2010JCLI3519.1

Tozuka T, Kataoka T, Yamagata T (2014) Locally and remotely forced atmospheric circulation anomalies of Ningaloo Niño/Niña. Clim Dyn 43:2197–2205. https://doi.org/10.1007/s00382-013-2044-x

Trenberth KE, Fasullo JT (2013) An apparent hiatus in global warming? Earth's Future 1:19–32. https://doi.org/10.1002/2013ef000165

Tsujino H et al (2018) JRA-55 based surface dataset for driving ocean—sea–ice models (JRA55-do. Ocean Model. https://doi.org/10.1016/j.ocemod.2018.07.002

Ummenhofer CC, Sen Gupta A, England MH, Taschetto AS, Briggs PR, Raupach MR (2015) How did ocean warming affect Australian rainfall extremes during the 2010/2011 La Niña event? Geophys Res Lett 42:9942–9951. https://doi.org/10.1002/2015GL065948

Wijffels S, Roemmich D, Monselesan D, Church J, Gilson J (2016) Ocean temperatures chronicle the ongoing warming of Earth. Nature Clim Change 6:116–118. https://doi.org/10.1038/nclimate2924

Yan X-H et al (2016) The global warming hiatus: Slowdown or redistribution? Earth's Future 4:472–482. https://doi.org/10.1002/2016EF000417

Zinke J et al (2015) Coral record of southeast Indian Ocean marine heatwaves with intensified Western Pacific temperature gradient. Nature Commun 6:8562. https://doi.org/10.1038/ncomms9562